

Study of mechanisms of nuclear-spin-wave relaxation in the weakly anisotropic antiferromagnet CsMnF₃

A. V. Andrienko, V. I. Ozhogin, V. L. Safonov, and A. Yu. Yakubovskii

I. V. Kurchatov Institute of Atomic Energy

(Submitted 24 July 1983)

Zh. Eksp. Teor. Fiz. **84**, 1158–1169 (March 1983)

The relaxation of parametric nuclear spin waves (NSW) in an easy-plane antiferromagnet are investigated in a wide frequency range $\nu_p = 2\nu_k = 600\text{--}1200$ MHz and at temperatures $T = 1.5\text{--}4.2$ K. It is found that at low temperatures ($T < 2.2$ K) the principal role is played by NSW scattering by fluctuations of the nuclear-magnetization components, a process whose contribution to the relaxation rate is $\Gamma_1 \propto T|\mathbf{k}|$. It is shown that this relaxation is practically independent of the NSW frequency and a model is proposed for explaining this behavior of the relaxation. At higher temperatures the main contribution to the relaxation rate is made by $\Gamma_2 \propto T^5|\mathbf{k}|$. A theoretical analysis and an investigation of the frequency dependence has made it possible to separate two relaxation processes, of which one (two-phonon, $\Gamma_{2ph} \propto T^5/k$) is the fundamental one at low frequencies, and the other, (two-magnon, $\Gamma_{2m} \propto T^5 H^2/k$) at high frequencies. The combination of these processes describes well the dependence of Γ_2 on the NSW frequency and of the value of their wave vector. In the frequency region $\nu_k = 350\text{--}450$ MHz the parametric excitation of the NSW was of the "hard" type.

PACS numbers: 76.50. + g, 75.50.Ee

INTRODUCTION

Hyperfine interaction between electron and nuclear spins in magnetically ordered dielectrics leads to two fundamental results. First, the magnetic moment of the electron shell, polarized by the exchange interaction, produces at the nucleus a strong magnetic field (~ 105 Oe) that determines the frequency of the free precession of the nuclear spin ω_n . Second, owing to the hyperfine interaction, a mixing of the oscillations of the electron and nuclear spins takes place. The oscillations of the nuclear magnetization, producing a relatively low-frequency perturbation on the line wing of the inhomogeneous resonance of the electron subsystem, can propagate in the crystal to considerable distances. An indirect coupling (the Suhl-Nakamura coupling¹) is thus produced between the nuclei and leads to correlation between their motion and in final analysis to the onset of collective oscillations. The excitations corresponding to these collective oscillations in the NMR frequency range were named nuclear spin waves (NSW). The most remarkable feature of NSW, which distinguishes them from ordinary spin waves, is that they exist in a paramagnetic system of nuclear spin waves that has at helium temperatures a high level of thermal fluctuations and a weak polarization ($\langle I \rangle / I \sim 1\%$). The concept of NSW was proposed in Ref. 2, where their spectra in ferro- and antiferromagnets were calculated, and where it was also predicted that the most convenient objects for the NSW study would be cubic antiferromagnets and antiferromagnets with easy-plane anisotropy (AFEP). This was followed by many experimental and theoretical studies of these interesting quasiparticles.^{3–13}

Several methods were used for the experimental study of NSW. The traditional NMR technique and spin-echo methods make it possible to excite NSW packets with wave vectors $|\mathbf{k}| \sim \Delta k \lesssim 10^4 \text{ cm}^{-1}$ (Δk is the width of the packet)

and to investigate their integral relaxation characteristics as a function of the temperature T and of the external magnetic field H . More information is provided by the method of parallel microwave pumping, in which are parametrically excited pairs of NSW with wave vectors \mathbf{k} and $-\mathbf{k}$ ($k = 10^5\text{--}10^6 \text{ cm}^{-1}$), with $\Delta k \ll k$. The threshold microwave-field amplitude h_c at which the parametric process begins yields direct information on the NSW relaxation frequency as a function of T , H , and k .

NSW has been the subject of a number of experimental and theoretical studies. Measurements were performed on ⁵⁵Mn nuclei in the AFEP CsMnF₃,^{4,5} MnCO₂,^{6–8} and in the cubic antiferromagnet RbMnF₃ (Ref. 9; see also the review¹⁰). The experimental picture of the behavior of the NSW relaxation in AFEP reduced to the following:

1) Two characteristic temperature dependences of the relaxation rate, $\Gamma \propto T$ at $T < 3$ K and $\Gamma \propto T^5$ at $T \gtrsim 3$ K were distinguished at helium temperatures NSW with wave vectors $|\mathbf{k}| \leq 10^5 \text{ cm}^{-1}$; on the other hand no dependence of Γ on k was observed.

2) It was found for NSW with $k \gtrsim 10^5 \text{ cm}^{-1}$ that at relatively low temperatures there exists a process with $\Gamma_1 \propto T|\mathbf{k}|$ against the background of which a process with $\Gamma_2 \propto T^{5-7}$ appears when the temperature is raised.

NSW relaxation was considered theoretically in Refs. 11 and 12, where the main NSW mechanisms were calculated within the framework of the two-sublattice model. These mechanisms described qualitatively (and in order of magnitude) the experimentally available data ($\Gamma_{1\text{theor}} \propto T|\mathbf{k}|$, $\Gamma_{2\text{theor}} \propto T^5/k$). The expressions obtained in Ref. 12 for the relaxations $\Gamma_{1\text{theor}}$ and $\Gamma_{2\text{theor}}$ depend strongly on the parameters of the NSW themselves, namely the wave vector \mathbf{k} and the frequency ν_k , but these dependences were either not confirmed in experiment (Γ_2 is independent of k in MnCO₃, Ref. 7), or were not investigated. To check on the correctness of

the theoretical premises of NSW relaxation it was necessary to measure the NSW frequencies in detail in a wide temperature range. The AFEP CsMnF₃ is the most convenient object for such investigations, since it is not subject to the Dzyaloshinskii interaction and NSW are therefore excited in it with frequencies 300–600 MHz at temperatures 1.5–4.2 K in fields $H > 0.6$ kOe, where the sample is known to be uniformly magnetized (this condition is satisfied in MnCO₃ only for NSW with frequency $\nu_k > 500$ MHz).

We used in our study a new modulation method of recording the microwave pump threshold. This method led to much more accurate measurements of the relaxation rate and yielded reliable information on the $\Gamma(T, k, \nu_k)$ dependence. A theoretical analysis was carried out in parallel with the experimental investigations.

PROCEDURE

Parametric NSW were excited by parallel microwave pumping in a wide frequency range $\nu_k = \nu_p/2 = 300$ –600 MHz and at temperatures 1.5–4.2 K. The CsMnF₃ sample measuring $4 \times 3 \times 2$ mm was placed at the center of a helical resonator of 8 mm diameter, having no coil form and capacitively coupled through posts at its end faces. At an input coupling close to critical, the loaded Q of the resonator at helium temperatures was $Q \sim 500$. The dc, microwave, and modulating magnetic fields were parallel to one another and were located in the basal plane of the crystal.

The traditional procedure of measuring NSW relaxation is the following.⁷ At a constant amplitude of the microwave field on the sample, an x - y recorder plots the microwave power passing through the resonator as a function of H . Starting with a certain amplitude, an absorption region appears on these curves and corresponds to parametric excitation of NSW. This excitation extends with increasing microwave power further towards weaker fields. Thus, for each value of H_c one can determine a corresponding amplitude of the microwave field h_c ; this amplitude is connected with the relaxation frequency of the excited NSW by the known formula¹³:

$$\Gamma = (H_c h_c / 2H_\Delta^2) (\nu_n^2 - \nu_k^2)^2 / \nu_k \nu_n^2. \quad (1)$$

The wave vector $|\mathbf{k}|$ of the excited NSW is calculated from the known NSW spectrum³

$$\nu_k = \nu_p/2 = \nu_n [1 - H_\Delta^2 / (H_c^2 + H_\Delta^2 + \alpha^2 k^2)]^{1/2}. \quad (2)$$

In these equations, $\nu_n = \omega_n/2\pi = 666$ MHz is the unshifted NMR frequency in CsMnF₃; $H_\Delta^2 = 6.4/T$ kOe² is the hyperfine interaction parameter; $\alpha = 0.95 \times 10^{-5}$ kOe-cm is the inhomogeneous exchange constant. In this procedure, the accuracy of the determination of H_c , is governed mainly by the sensitivity of the apparatus, since H_c is taken to be the field at which the absorption signal exceeds the system noise. As seen from (1) and (2), the error in the determination of H_c influences significantly not only the calculated value of αk , but also the obtained value of Γ ; this can lead to a strong distortion of the $\Gamma(\mathbf{k})$ dependence. Therefore the question of raising the sensitivity and consequently of a more accurate measurement of H_c becomes basic in experiments on the

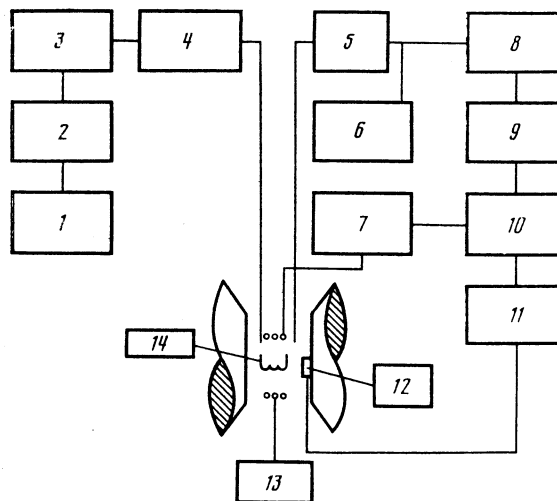


FIG. 1. Block diagram of experimental setup for the investigation of NSW relaxation: 1—G4-37A generator, 2—D2-13 attenuator, 3—SWR meter, 4—variable-length line; 5—gate, 6—S4-40 spectrum analyzer; 7—G3-33 modulation generator; 8—P5-20 receiver (replaced by a crystal detector outside the P5-20 receiver frequency range, i.e., at $\nu_p > 1040$ MHz); 9—V6-9 tuned amplifier; 10—SD-1 synchronous detector; 11—PDP4-002 automatic recorder; 12—Hall pickup; 13—modulation coil; 14—resonator.

study of NSW relaxation by observing the threshold of the parallel microwave pumping. The sensitivity reached in Ref. 7 is apparently close to the limit for measurements without modulation.

To record the field H_c corresponding to the start of the parametric excitation of the NSW, we have used a modulation procedure (see the block diagram of Fig. 1) which makes it possible to improve the sensitivity appreciably. The modulating field H_m at the sample was produced by a coil of 2 cm diameter placed coaxially with the helical resonator. The modulation frequency $F = \omega/2\pi = 100$ kHz and the amplitude $H_m < 0.07$ Oe were chosen such that the influence of the modulation on the pump threshold be negligibly small.¹⁴ Directly above the threshold, amplitude modulation of the microwave signal passing through the microwave resonator sets in, is separated by a synchronous-detector system and is recorded with an x - y plotter. Typical experimental plots of this signal A_F are shown in Fig. 2. The signal/noise ratio on curve 3 corresponds approximately to that reached in Ref. 7. With increasing gain of the system, the parametric instability onset registered in the experiment shifts towards weaker fields and reaches the value H_c^* . Since further increase of the insensitivity does not lead to a change of H_c (see curves 2 and 1), it is natural to assume H_c^* to be the true start of the parametric excitation of the NSW.

The absolute error in the determination of h_c by any recording procedure is relatively large ($\pm 25\%$), since it is due to the errors in the measurement of the microwave power, of the coefficient β of coupling to the cavity, and of the Q of the latter (an additional error is due to the insufficiently well known distribution of the microwave field inside and outside the helix). For a comparison of the experimental functional dependences of the relaxation rate Γ at a fixed pump frequency with the theory, the absolute error does not

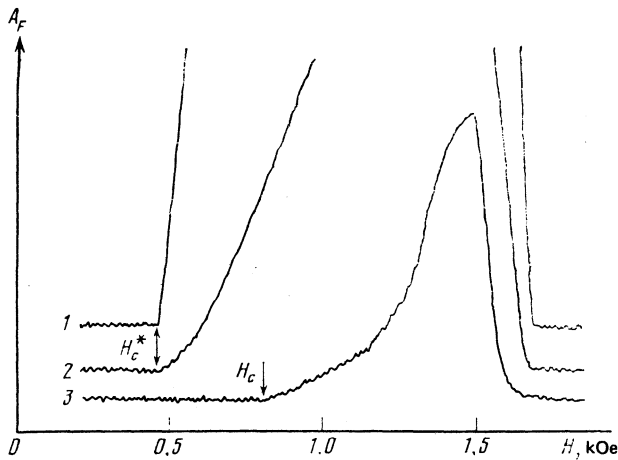


FIG. 2. Experimental plots of the component A_F of the signal passing through the resonator as a function of H . Curve 1 corresponds to the maximum sensitivity of the circuit, and curve 2 was obtained with the sensitivity decreased by a factor 10, while curve 3 was obtained with the sensitivity decreased by another factor 30 (300 times the maximum value).

play a major role, and the relative error, determined by the stability of the microwave generator level and by the accuracy of the attenuator calculation, does not exceed 2% in our case.

NSW RELAXATION

Figure 3 shows a typical plot of the NSW relaxation vs the wave vector in coordinates $(\Gamma/T, \alpha k)$ at a fixed pump frequency $\nu_p = 1128$ MHz. The choice of the coordinates makes it possible to separate all corrections to the principal low-temperature relaxation mechanism, $\Gamma_1 \propto T|\mathbf{k}|$. At temperatures $T \leq 2.2$ K the experimental points plotted in these coordinates lie on one straight line passing through the origin.

With further increase of the temperature, the experimental points begin to deviate from the straight line de-

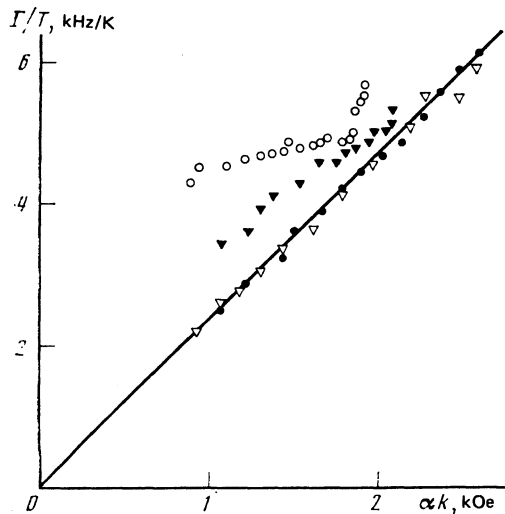


FIG. 3. Experimental behavior of the NSW relaxation wave in the coordinates Γ/T and αk at a pump frequency $\nu_p = 1128$ MHz and at several temperatures: \circ —4.23 K; \blacktriangledown —3.45 K; ∇ —2.13; \bullet —1.70 K.

scribed above (see Fig. 3). This is evidence of an additional contribution to the total relaxation from another mechanism with essentially different dependences on \mathbf{k} and T . Subtracting from the total relaxation Γ the corresponding values of Γ_1 we obtain the relaxation rate Γ_2 for this additional process. It must be noted that at small values of the wave vector $k < k^*$ the relaxation Γ ceases to depend on k (when the pump frequency increases from 600 to 1200 MHz, k^* increases from 0.5×10^5 to 10^5 cm^{-1}). This is the region of the so-called inhomogeneous broadening, previously observed in MnCO_3 (Refs. 6 and 7) and in RbMnF_3 (Ref. 9). We analyze below experimental results obtained only in the region $k > k^*$.

We consider first the process with the linear dependence of the relaxation on the temperature and on the wave vector, $\Gamma_1 \propto T|\mathbf{k}|$. It was shown in Ref. 11 that such a dependence is due to elastic scattering of the NSW by the fluctuations of the longitudinal component of the nuclear magnetization (the calculation was made under the assumption that $\nu_n - \nu_k \ll \nu_n$). This mechanism was later calculated for arbitrary ν_k (Ref. 12) and a frequency dependence $\Gamma_1 \propto \nu_k^3$ was obtained.

Our first measurements of the NSW relaxation in a wide frequency band have shown, however, that within the limits of the measurement accuracy the relaxation Γ_1 does not depend on the frequency ν_k (Fig. 4). At any rate it is obvious that the dashed theoretical $\Gamma_1 \propto \nu_k^3$ curve in Fig. 4 does not describe the experimental data. This discrepancy is probably due to the fact that the heuristic approach used in Ref. 12 and based on the Holstein-Primakoff expansion does not take into account with sufficient rigor the thermal fluctuations of the nuclear spins. Naturally, a more rigorous conclusion must be obtained within the framework of the spin representation. Using the diagrammatic technique of spin operators for the scattering of NSW by fluctuations of nuclear spins, we can obtain the following expression for the NSW relaxation rate (see Appendix A):

$$\Gamma_1 = \frac{\nu_n}{8\pi} \frac{(1+\xi^2)^2}{4\xi} (V_0^{1/2} k) \frac{T}{\Theta_N} \frac{J_0}{k_B \Theta_N}. \quad (3)$$

Here $\xi = \nu_k/\nu_n$, V_0 is the unit-cell volume, $\Theta_N = g\mu_B \alpha / V_0^{1/3} / k_B$, J_0 is the energy of exchange interaction

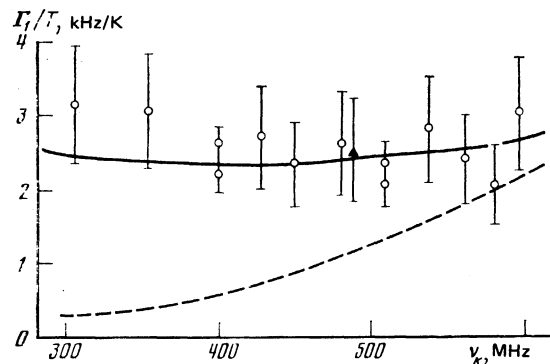


FIG. 4. Frequency dependence of the relaxation Γ_1/T at $\alpha k = 1$ kOe ($k \approx 1.05 \cdot 10^5$ cm^{-1}). Dashed curve—theoretical relation obtained in Ref. 12; solid—calculation by Eq. (3) of the present paper; \blacktriangle —data of Ref. 4.

of the neighboring electron spins, and k_B is the Boltzmann constant. As $\nu_k \rightarrow \nu_n$ expression (3) coincides with the Richards formula.¹¹ The theoretical frequency dependence of Γ_1 shown in Fig. 4 (solid line) agrees well with the experimental one. Estimate (3) at typical values of the parameters of CsMnF_3 ($J_0/k_B \approx 19$ K, $\Theta_N \approx 29$ K, $V_0 \approx 0.84 \cdot 10^{-22}$ cm³) is in good qualitative agreement with the observed values of the NSW relaxation, namely:

$$\Gamma_{1\text{theor}}[\text{kHz}] \approx 2.6 \frac{(1+\xi^2)^2}{4\xi} k [10^5 \text{ cm}^{-1}] T [\text{K}],$$

whereas the experimental results (Fig. 4) are described by the same dependence on T , k , and ξ , with a numerical coefficient 2.9 ± 0.7 .

We now subtract from the total relaxation Γ the value $\Gamma_1(T, k, \xi)$ and consider the remaining relaxation Γ_2 . Figure 5 shows its temperature dependence at the frequency $\nu_p = 2\nu_k = 904$ MHz at $\alpha k = 0.9$ kOe. A similar picture is observed also at other values of ν_k and αk . The experimental results are well described by the relation $\Gamma_2 \propto T^{5 \pm 0.5}$. A detailed theoretical analysis of the possible intrinsic relaxation processes, given in Ref. 12, has shown that the only possible explanation of the $\Gamma \propto T^5$ dependence in a two-sublattice antiferromagnet is the interaction of the NSW with two thermal phonons (we shall call this hereafter two-phonon interaction), for which

$$\Gamma_{2ph} = \frac{\pi^2}{20I(I+1)} (1-\xi^2)^2 \left(\frac{k_B \tilde{\Theta}}{Mv_s^2} \right)^2 \left(\frac{k_B}{\hbar} \right)^2 \frac{T^5}{\Theta_D^3 v_s k}. \quad (4)$$

Here M is the mass of the unit cell; v_s is the speed of sound, and $\Theta_D = \hbar v_s / V_0^{1/3} k_B$. Expression (4) contains the constant $\tilde{\Theta} \propto B^{(2)}$ which characterizes the energy of the relativistic second-order interaction described by the term $B^{(2)} L^2 u^2$ in the total Hamiltonian; the value of this constant for CsMnF_3 is unknown. In order that the estimate Γ_{2ph} (at $v_s \approx 2.3 \times 10^5$ cm/sec; $Mv_s^2/k_B \approx 1.6 \cdot 10^5$ K; $\Theta_D \approx$ K) agree with the obtained experimental data it is necessary to have $\tilde{\Theta} \sim 10^{2-3}$ K. This estimate for $\tilde{\Theta}$ is perfectly realistic, since it can be as-

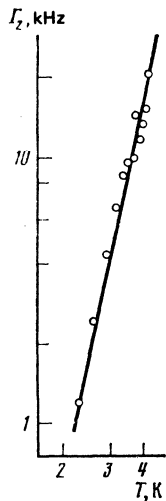


FIG. 5. Temperature dependence of the relaxation Γ_2 for $\nu_p = 904$ MHz at $\alpha k = 0.9$ kOe ($k \approx 0.95 \times 10^5$ cm⁻¹).

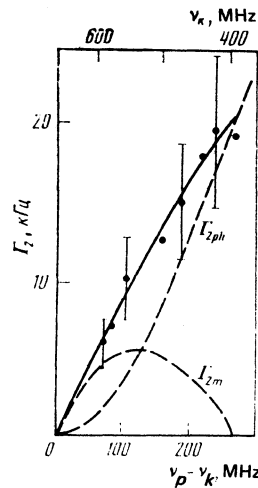


FIG. 6. Frequency dependence of the relaxation Γ_2 at $T = 4.2$ K, $\alpha k = 0.9$ kOe ($k \approx 0.95 \cdot 10^5$ cm⁻¹). The dashed lines show the frequency dependences for two-phonon Γ_{2ph} (Ref. 12) and two-magnon Γ_{2m} [Eq. (5)] relaxation processes. The solid line is a linear combination of these processes (6), which describes best the experimental data.

sumed that $B^{(2)} \sim 10 - 100 B^{(1)}$ (Ref. 15), and for AFEP the first-order magnetoelastic constants are $\Theta \sim 1 - 10$ K. (A comparison of the heights of the peaks on the plots of the spin-wave relaxations vs the magnetic field at the points of intersection of the magnon and phonon branches in CsMnF_3 (Ref. 16) and MnCO_3 (Ref. 17) shows that the magnetoelastic coupling in these AFEP are of the same order, and it is known that $\Theta \approx 3$ K¹⁸ for MnCO_3 .)

Figure 6 shows the dependence of the relaxation parameter Γ_2 on the NSW frequency at $T = 4.22$ K and $\alpha k = 0.9$ kOe.¹ It can be seen that the theoretical dependence of the two-phonon process Γ_{2ph} (Ref. 12) does not make it possible to describe the experimental data in the entire frequency range. This circumstance has stimulated searches for an NSW relaxation mechanism having the same temperature dependence as $\Gamma_{2ph} (\propto T^5)$, but with a substantially different dependence on the NSW frequency. Such a mechanism should (by itself or in conjunction with the already calculated Γ_{2ph}) describe the experimental frequency dependence $\Gamma_2(\nu_k)$. A detailed theoretical analysis has shown that there is no such mechanism within the framework of the two-sublattice model of an antiferromagnet.

Using neutron-diffraction data¹⁹ for CsMnF_3 , we have calculated the nuclear-spin oscillations within the framework of the six-sublattice model of an antiferromagnet (the details of the calculations will be published in a separate paper). A theoretical analysis has shown that the expressions for the spectrum and for the NSW relaxation frequencies in a six-sublattice model differ from the analogous expression in the two-sublattice model of an antiferromagnet, but to the extent that in the interval between the two unshifted NMR frequencies ($\nu_{1n} = 666$ MHz, $\nu_{2n} = 676$ MHz) the difference amounts to $\sim 1\%$. A detailed examination, however, has shown that besides the spin-wave interaction processes peculiar to the two-sublattice antiferromagnet, in the microscopic six-sublattice model the exchange-interaction Hamiltonian leads to a new type of spin anharmonicity—interac-

tion processes with participation of three magnons of only the quasiferromagnetic (f) branch of the spectrum (and accordingly interactions of the NSW with the quasiferromagnons—see Appendix B).²⁾ This difference is due to the fact that the local symmetry of the two nonequivalent positions of the Mn^{2+} ions ($Mn I - D_{3d}$, $Mn II - C_{3v}$) in the unit cell is lower than the symmetry of the cell as a whole (D_{6h}) (see e.g., Ref. 21). It turns out as a result that the coordinate sums over the nearest neighbors do not coincide for different magnetic ions, so that in the presence of shear of the magnetic sublattices on account of an external magnetic moments, a new type of three-magnon interactions appears in the magnon quasi-antiferromagnetic branch of the spectrum besides the usual three-particle interactions of two f -magnons. Without presenting the cumbersome calculations, we write down for the NSW relaxation parameter an expression determined by the process of coalescence of an NSW with an f magnon into an f magnon (hereafter called two-magnon process):

$$\Gamma_{2m} = C_{2m} (1 - \xi^2)^2 \frac{g\mu_B H}{\hbar} \frac{H}{\alpha k} \left(\frac{T}{\Theta_N} \right)^5, \quad C_{2m} \sim 10^{-3}. \quad (5)$$

An estimate of (5) at typical values of the parameters agrees in order of magnitude with the experimental data at frequencies $\nu_k \gtrsim 550$ MHz.

According to (5), the two-magnon process of NSW relaxation depends on the frequency and wave vector of the NSW in a manner different from the two-phonon process (4) (dashed lines in Fig. 6). Taken separately, however, the two-magnon relaxation process, just as the two phonon one, cannot describe the behavior of Γ_2 in the entire range of pump frequencies. In contrast to Γ_{2ph} , $\Gamma_{2m}(\nu_k)$ makes it possible to describe the experimental results in the limit of high NSW frequency. Thus, the experimental frequency dependence of $\Gamma_2(\nu_k)$ can be described only by a combination of both considered NSW-relaxation processes—the two-phonon (4) and the two-magnon (5). The solid curve in Fig. 6 corresponds to the sum of the two process (Γ_{2ph} and Γ_{2m}):

$$\Gamma_2 [\text{MHz}] = [1 - (\nu_k/\nu_n)^2]^2 \{3.3 + 1.6 (H [\text{kOe}])^2\} (T [\text{K}])^5 / k [\text{cm}^{-1}]. \quad (6)$$

The numerical coefficients in (6) were chosen such as to describe in best fashion the experimental frequency dependence. They correspond to $\bar{\Theta} \approx 1.1 \cdot 10^3$ K and $C_{2m} \approx 3.7 \cdot 10^{-3}$. Thus, at low frequencies we should have $\Gamma_2 \approx \Gamma_{2ph} \propto 1/k$. Actually the experimental data at frequencies $\nu_k \lesssim 450$ MHz are satisfactorily described by the expression $\Gamma_2 \propto 1/k$. At higher frequencies, at the same time, $\Gamma_2(k)$ has a more complicated form, since the contribution from the process $\Gamma_{2m} \propto H^2/k$ becomes noticeable. Figure 7 shows the experimental values of $\Gamma_2(k)$ for $\nu_p = 1128$ MHz at two temperatures. The solid lines are the result of calculation by Eq. (6). Thus, the linear combination (6) of the processes Γ_{2ph} and Γ_{2m} permits a good description of the experimental plots of the relaxation Γ_2 in CsMnF_3 vs the NSW frequency, and of the value of their wave vector.

The experimental data of Refs. 6 and 7 indicate that in

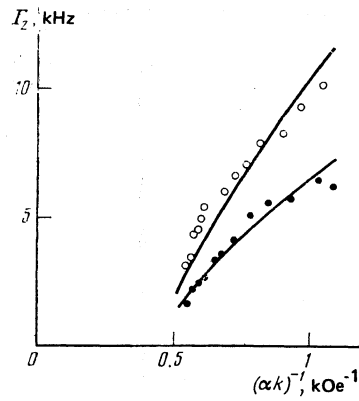


FIG. 7. Relaxation Γ_2 vs the reciprocal of the wave vector for $\nu_p = 1128$ MHz: light circles— $T = 4.24$ K; dark circles— $T = 3.88$ K. Solid lines—result of calculation by Eq. (6).

the two-sublattice antiferromagnet MnCO_3 the process $\Gamma_2 \propto T^{5-7}$ does not depend on the value of the wave vector. This circumstance is apparently connected with the presence of defects in the investigated samples. Owing to the imperfection of the lattice, particle interaction processes without conservation of the quasimomentum are possible, therefore the $\Gamma_{2ph} \propto 1/k$ relation can become considerably weaker in the region $k \lesssim l_{im}^{-1}$ (l_{im} is the characteristic distance between defects).

In the range of low frequencies, $\nu_k = 350-450$ MHz there is observed a "hard" character of parametric excitation of NSW: the onset and termination of the parametric process took place at different values of the limiting field H_c (see Fig. 2). This phenomenon was particularly strongly pronounced at the minimum temperature $T = 1.5$ K at the frequency $\nu_k \approx 400$ MHz. A noticeable increase of the above-threshold susceptibility χ'' of the sample was simultaneously observed. When the microwave power passing through the resonator was recorded, the curves on the plotter were similar to the $A_F(H)$ curves shown in Fig. 2.

The difference ($\Delta\Gamma$) between the relaxation rates obtained with increasing and decreasing field H , i.e., the eliminated part of the relaxation, was independent of k , increased with decreasing temperature like $\Delta\Gamma \propto T^{-1}$, and reached $\sim 30\%$ of the total relaxation Γ at $T = 1.5$ K. The hardness of the parametric excitation, long known for electronic magnons,²² was not observed previously in an NSW system.

APPENDIX A

The Hamiltonian of the interaction of the nuclear spins with spin waves of the lower (quasiferromagnetic) branch of the spectrum, determined by the hyperfine interaction, can be represented in the form²³

$$\begin{aligned} \mathcal{H}_{n-f} = & N^{-1/2} \sum_{\mathbf{k}} \frac{\omega_n}{2} \left(\frac{\hbar J_0}{2\omega_{f\mathbf{k}}} \right)^{1/2} (c_{\mathbf{k}} - c_{-\mathbf{k}}^{\dagger}) (m_{\mathbf{k}} - m_{-\mathbf{k}}^{\dagger}) \\ & - N^{-1} \sum_{\mathbf{k}, \mathbf{q}} \frac{J_0 \omega_{\mathbf{k}}}{4(\omega_{f\mathbf{k}} \omega_{f\mathbf{q}})^{1/2}} (c_{\mathbf{k}} - c_{-\mathbf{k}}^{\dagger}) (c_{\mathbf{q}} - c_{-\mathbf{q}}^{\dagger}) \Delta m_{\mathbf{k}+\mathbf{q}}^{\dagger}. \quad (\text{A1}) \end{aligned}$$

Here $c_{\mathbf{k}}^{\dagger}$ and $c_{\mathbf{k}}$ are the f -magnon creation and annihilation

operators, $m_k^\alpha = I_{1k}^\alpha + I_{2k}^\alpha$, I_{jk}^α are the Fourier components of the nuclear spins of the two sublattices ($j = 1, 2$; $\alpha = \pm, z$). Since the NSW frequencies lie much lower than the bottom of the quasi-ferromagnetic (f) branch of the spectrum ($\omega_n \ll \omega_{f0}$), to describe the interactions inside the system of nuclear spins it is convenient to change over to an effective Hamiltonian of indirect interactions, by averaging the high-frequency oscillations of the electronic spins:

$$\mathcal{H}_{eff} = \text{Sp} [\exp(-\beta \mathcal{H}_{of}) \mathcal{H} \sigma(\beta)] / \text{Sp} [\exp(-\beta \mathcal{H}_{of}) \sigma(\beta)], \quad (\text{A2})$$

$$\mathcal{H}_{of} = \sum_{\mathbf{k}} \hbar \omega_{f\mathbf{k}} c_{\mathbf{k}}^+ c_{\mathbf{k}},$$

where $\sigma(\beta)$ is the temperature scattering matrix. In the up-shot,

$$\begin{aligned} \mathcal{H}_{eff} = & N^{-1} \sum_{\mathbf{k}} V_{\mathbf{k}} (m_{\mathbf{k}}^- - m_{-\mathbf{k}}^+) (m_{-\mathbf{k}}^- - m_{\mathbf{k}}^+) \\ & + N^{-2} \sum_{\mathbf{k}, \mathbf{q}} U_{\mathbf{k}, \mathbf{q}} (m_{\mathbf{k}}^- - m_{-\mathbf{k}}^+) (m_{\mathbf{q}}^- - m_{-\mathbf{q}}^+) \Delta m_{\mathbf{k}+\mathbf{q}}^+; \end{aligned} \quad (\text{A3})$$

$$V_{\mathbf{k}} = \frac{J_0}{8} \left(\frac{\omega_n}{\omega_{f\mathbf{k}}} \right)^2, \quad U_{\mathbf{k}, \mathbf{q}} \approx -\frac{4}{\hbar \omega_n} V_{\mathbf{k}} V_{\mathbf{q}}.$$

The first term in (A3) describes the Suhl-Nakamura interaction,² and the second the indirect three-spin interaction.²⁴

The Hamilton \mathcal{H}_{eff} in conjunction with the Hamiltonian of the free precession of the nuclear spins in the hyperfine-interaction spin,

$$\mathcal{H}_{on} = -\hbar \omega_n m_0^z, \quad (\text{A4})$$

can be diagonalized by the canonical transformation²⁵:

$$\tilde{\mathcal{H}} = Q (\mathcal{H}_{on} + \mathcal{H}_{eff}) Q^{-1}, \quad (\text{A5})$$

$$Q = \exp \left\{ N^{-1} \sum_{\mathbf{k}} \frac{1}{46b} \ln \frac{\omega_n}{\omega_{\mathbf{k}}} (m_{\mathbf{k}}^- m_{-\mathbf{k}}^- - m_{\mathbf{k}}^+ m_{-\mathbf{k}}^+) \right\};$$

$b = IB_I (\hbar \omega_n / k_B T)$; $B_I(x)$ is the Brillouin function. As a result we have

$$\begin{aligned} \tilde{\mathcal{H}} = & -\hbar \omega_n m_0^z + N^{-1} \sum_{\mathbf{k}} \tilde{V}_{\mathbf{k}} m_{\mathbf{k}}^+ m_{-\mathbf{k}}^- + N^{-2} \sum_{\mathbf{k}, \mathbf{q}} \tilde{U}_{\mathbf{k}, \mathbf{q}} m_{\mathbf{k}}^+ m_{\mathbf{q}}^- \Delta m_{-\mathbf{k}+\mathbf{q}}^-; \\ \tilde{V}_{\mathbf{k}} = & \hbar (\omega_{\mathbf{k}} - \omega_n) / 4b; \end{aligned} \quad (\text{A6})$$

$$\begin{aligned} \tilde{U}_{\mathbf{k}, \mathbf{q}} = & \hbar \omega_n / 8b^2 - 2U_{\mathbf{k}, \mathbf{q}} \omega_n / (\omega_{\mathbf{k}} \omega_{\mathbf{q}})^{1/2} \\ & + [f(\mathbf{k}, \mathbf{q}) - f(\mathbf{q}, \mathbf{k})] / 16b^2 \ln (\omega_{\mathbf{k}} / \omega_{\mathbf{q}}); \\ f(\mathbf{k}, \mathbf{q}) = & \hbar [2\omega_{\mathbf{q}} + (\omega_n^2 - \omega_{\mathbf{q}}^2) / (\omega_{\mathbf{k}} \omega_{\mathbf{q}})^{1/2}] \ln (\omega_n / \omega_{\mathbf{k}}). \end{aligned}$$

Using the spin-operator diagrammatic technique,²⁶ we can easily write down a formula for the NSW damping decrement due to the scattering of the NSW by the thermal fluctuations of the nuclear spins:

$$\gamma_1 = 2^3 b' \pi V_0 \int \frac{d\mathbf{q}}{(2\pi)^3} |\tilde{V}_{\mathbf{q}} + 2b \tilde{U}_{\mathbf{k}, \mathbf{q}}|^2 \delta(\omega_{\mathbf{k}} - \omega_{\mathbf{q}}), \quad (\text{A7})$$

$$b' = \frac{k_B T}{\hbar} \frac{db}{d\omega_n}.$$

Following a direct calculation we obtain in the limit $T \gg \hbar \omega_n / k_B$ expression (3).

APPENDIX B

Analysis shows that in the six-sublattice model of CsMnF₃ the three-magnon processes are determined mainly by the exchange interactions $J_{16} = J_{45} = J_{34} = J_{12} = J_1$, $J_1 / k_B \approx 6.5$ K (Ref. 19). The resultant amplitudes of the interaction with participation of three f magnons are governed by the fact that the coordination sums $Z^\pm(\mathbf{q})$ are different for different positions of the Mn²⁺ ions in the following expression:

$$\mathcal{F}(\mathbf{k}_1, \mathbf{k}_2, \mathbf{k}_3) = \sum_{j=1}^3 [Z^+(\mathbf{k}_j) - Z^-(\mathbf{k}_j)] \Delta(\mathbf{k}_1 + \mathbf{k}_2 - \mathbf{k}_3), \quad (\text{B1})$$

where

$$\begin{aligned} Z^\pm(\mathbf{q}) = & \cos[(\mathbf{n}_1 + \mathbf{n}_2 \mp \mathbf{n}_3) \mathbf{q}] + \cos[(-\mathbf{n}_1 + \mathbf{n}_2 \pm \mathbf{n}_3) \mathbf{q}] \\ & + \cos[(\pm 2\mathbf{n}_2 + \mathbf{n}_3) \mathbf{q}]. \end{aligned} \quad (\text{B2})$$

Here $\mathbf{n}_1 = \mathbf{a}/2$, $\mathbf{n}_2 = \mathbf{b}/3 + \mathbf{a}/6$, $\mathbf{n}_3 = u\mathbf{c}$, $u \approx 0.15$ ($\mathbf{a}, \mathbf{c}, \mathbf{b} || [\mathbf{c} \times \mathbf{a}]$ is the basis of the cell).

Recognizing that when account is taken of the hyperfine interaction the f magnons contain an admixture of nuclear-spin oscillations, we can obtain the amplitude for the interaction of NSW with two f magnons:

$$\Psi_{n,2f} \propto \mathcal{F}(\mathbf{k}, \mathbf{q}, \mathbf{k}+\mathbf{q}) \frac{(g\mu_B)^2 H_\Delta H \omega_n (SJ_1)^{1/2}}{\hbar^{3/2} \omega_{\mathbf{k}}^2 (\omega_{\mathbf{k}} \omega_{\mathbf{q}} \omega_{\mathbf{k}+\mathbf{q}})^{1/2}}. \quad (\text{B3})$$

The authors thank A. S. Borovik-Romanov, B. Ya. Kolyuzhanskiĭ, V. S. Lutovinov, L. A. Prozorova, and M. A. Savchenko for helpful discussions.

¹For this value of αk it is possible to investigate the $\Gamma_2(\nu_{\mathbf{k}})$ dependence in the widest frequency range.

²We note that in the two-sublattice model the processes with interaction of three f magnons are possible only when account is taken of the relativistic interactions (dipole-dipole etc.), whose contribution to the NSW relaxation is negligibly small.

¹H. Suhl, Phys. Rev. **109**, 606 (1958). T. Nakamura, Progr. Theor. Phys. **20**, 542 (1958).

²P. G. de Gennes, P. A. Pincus, F. Hartmann-Boutron, and J. M. Winter, Phys. Rev., **129**, 1105 (1963).

³E. A. Turov and M. P. Petrov, Nuclear Magnetic Resonance in Ferro- and Antiferromagnets, Wiley, 1972.

⁴B. T. Adams, L. W. Hinderks, P. M. Richards, J. Appl. Phys. **41**, 931 (1970). L. W. Hinderks and P. M. Richards, *ibid.* **42**, 1516 (1971).

⁵A. Yu. Yakubovskii and S. M. Suleĭmanov, Zh. Eksp. Teor. Fiz. **81**, 1456 (1981) [Sov. Phys. JETP **54**, 772 (1981)].

⁶A. Yu. Yakubovskii, Zh. Eksp. Teor. Fiz. **67**, 1539 (1974) [Sov. Phys. JETP **40**, 766 (1975)].

⁷S. A. Govorkov and V. A. Tul'in, Zh. Eksp. Teor. Fiz. **73**, 1053 (1977) [Sov. Phys. JETP **46**, 558 (1977)].

⁸Yu. M. Bun'kov and B. S. Dumesh, Zh. Eksp. Teor. Fiz. **68**, 1161 (1975) [Sov. Phys. JETP **41**, 576 (1975)].

⁹S. A. Govorkov and V. A. Tul'in, Zh. Eksp. Teor. Fiz. **74**, 389 (1978) [Sov. Phys. JETP **47**, 202 (1978)].

¹⁰V. A. Tul'in, Fiz. Nizk. Temp. **5**, 965 (1979) [Sov. J. Low Temp. Phys. **5**, 455 (1979)].

¹¹P. M. Richards, Phys. Rev. **173**, 581 (1968).

¹²V. S. Lutovinov and V. L. Safonov, Fiz. Tverd. Tela (Leningrad) **21**, 2772 (1979) [Sov. Phys. Solid State **21**, 1594 (1979)].

¹³V. I. Ozhogin and A. Yu. Yakubovskii, Zh. Eksp. Teor. Fiz. **67**, 287 (1974) [Sov. Phys. JETP **40**, 144 (1975)].

¹⁴V. I. Ozhogin, A. Yu. Yakubovskii, A. V. Abryutin, and S. M. Suleĭmanov, Zh. Eksp. Teor. Fiz. **77**, 2061 (1979) [Sov. Phys. JETP **50**, 984 (1979)].

¹⁵A. N. Grishmanovskii, V. V. Lemanov, G. A. Smolenskii, A. M. Balbashov and A. Ya. Chervonenkis, Fiz. Tverd. Tela (Leningrad) **16**, 1426

- (1974) [Sov. Phys. Solid State **16**, 916 (1974)].
- ¹⁶M. H. Seavey, Phys. Rev. Lett. **23**, 132 (1969).
- ¹⁷V. V. Kveder, B. Ya. Kotyuzhanskii, and L. A. Prozorova, Zh. Eksp. Teor. Fiz. **63**, 2205 (1972) [Sov. Phys. JETP **36**, 1165 (1973)]. B. Ya. Kotyuzhanskii and L. A. Prozorova, *ibid.* **65**, 2470 (1973) [**38**, 1233 (1974)].
- ¹⁸V. R. Gakel', Zh. Eksp. Teor. Fiz. **67**, 1827 (1974) [Sov. Phys. JETP **40**, 908 (1975)].
- ¹⁹D. Khatamian and M. F. Collins, Canad. J. Phys. **55**, 773 (1977).
- ²⁰V. S. Lutovinov and V. L. Safonov, Fiz. Tverd. Tela (Leningrad) **24**, 1455 (1982) [Sov. Phys. Solid State **24**, 828 (1982)].
- ²¹V. V. Eremenko, Vvedenie v opticheskuyu spetskropiyu magnetikov (Introduction to Optical Spectroscopy of Magnets), Naukova dumka, 175, p. 197.
- ²²H. le Gall, B. Lemainre, and D. Sere, Sol. St. Commun. **5**, 919 (1967).
- ²³V. S. Lutovinov and V. L. Safonov, Fiz. Tverd. Tela (Leningrad) **23**, 2759 (1981) [Sov. Phys. Solid State **23**, 1615 (1981)].
- ²⁴N. N. Evtikhiev, V. S. Lutovinov, M. A. Aavchenko, and V. S. Safonov, Pis'ma Zh. Tekh. Fiz. **6**, 1527 (1980) [Sov. Tech. Phys. Lett. **6**, 659 (1980)].
- ²⁵V. L. Safonov, IAE Preprint No. 3691/1, 1982.
- ²⁶Yu. A. Izyumov, F. A. Kassan-ogly, and Yu. N. Skryabin, Polevye metody v teorii ferromagnetizma (Field Methods in Ferromagnetism Theory), Nauka, 1974, Chap. II.

Translated by J. G. Adashko